Received: 5 August 2020 | Revised: 18 September 2020 | Accepted: 16 October 2020

DOI: 10.1002/qua.26526

FULL PAPER

International Journal of QUANTUM CHEMISTRY WILEY

Unusual substituent effects in the Tr···Te triel bond

Ruijing Wang[1] | Canlin Luo[1] | Qingzhong Li[1] | Steve Scheiner[2]

[1]The Laboratory of Theoretical and Computational Chemistry, School of Chemistry and Chemical Engineering, Yantai University, Yantai, People's Republic of China

[2]Department of Chemistry and Biochemistry, Utah State University, Logan, Utah

Correspondence
Qingzhong Li, The Laboratory of Theoretical and Computational Chemistry, School of Chemistry and Chemical Engineering, Yantai University, Yantai 264005, People's Republic of China.
Email: liqingzhong1990@sina.com
Steve Scheiner, Department of Chemistry and Biochemistry, Utah State University, Logan, UT 84322-0300, USA.
Email: steve.scheiner@usu.edu

Funding information
National Natural Science Foundation of China, Grant/Award Number: 21573188; Science and Technology Innovation Fund of Yantai University, Grant/Award Number: YDZD2011

Abstract

The triel bond between the π-hole on the triel atom of TrR_3 (Tr = B, Al, Ga; R = H, F, Cl, Br) and a lone pair on the Te atom of H_2Te is examined using ab initio methods. For Tr = B, the triel bond is weakened as the R substituent becomes more electronegative, while the opposite pattern is noted for Al and Ga. The weakest triel bond of all occurs in H_2Te-BF_3 (2.9 kcal/mol) but is much stronger for all the other complexes (>11 kcal/mol). The placement of electron-releasing OH, NH_2, and CH_3 R′ substituents on the R'_2Te base strengthens the triel bond, whereas the opposite occurs for the electron-withdrawing CN. Despite its high electronegativity, the F substituent causes a strengthening of the interaction, which is due in large part to the formation of secondary chalcogen bonds that involve the σ-holes on Te in F_2Te. However, the F atom on TrF_3 is unable to act as an electron donor in these chalcogen bonds, leading to weakened F_2Te···TrF_3 interactions.

KEYWORDS
energy decomposition, noncovalent bond, triel bond, π-hole, σ-hole

1 | INTRODUCTION

The triel bond (TrB) is an attractive interaction between a group 13 (triel) atom and an electron donor. [1] A sp^2-hybridized Tr atom is electron-deficient and so can act as a Lewis acid in a complex with a base, [2] which is aided by a π-hole, [3] a region of positive electrostatic potential above a portion of a planar molecular framework. TrBs are typically quite strong and involve a certain degree of geometrical deformation of the triel-containing molecule. [4] While the π-hole is suggestive of a strong electrostatic component in the interaction, polarization also plays a prominent role. Like the hydrogen bond, the TrB has potential applications in chemical reactions. [5–7] A triel-bonded complex may be conceptualized as a transition state in S_N2 reactions, such as that between borine carbonyl (CO-BH_3) and trimethylamine, [5,6] as well as the borate-fluorine bond cleavage reaction by electron-rich late-transition metal complexes. [7] These and other applications have inspired some of the research into TrBs. [8–10]

The TrB shows some similarities with hydrogen and halogen bonds. Charge is transferred from the electron donor to the triel/hydrogen/halogen donor, that is, the Lewis acid. Electron-releasing substituents on the electron donor strengthen these interactions, as do electron-withdrawing substituents on the acid. It has been found that the Tr atom adjoined with an sp-hybridized carbon engages in a stronger TrB than that with sp^2 or sp^3-hybridized carbons. [11] The TrB displays cooperativity with itself and other types of interactions, by which the TrB strength can be increased or weakened. [12–14] For instance, both TrB and regium bond are strengthened in a ternary complex such as C_2H_4-MCN-TrR_3 (M = Cu, Ag, Au; Tr = B, Al; R = H, F). [13]

Despite these similarities, the TrB displays some intriguing differences with hydrogen and halogen bonds. For example, the electron-releasing methyl group seems to have differing effects on the two types of interactions. [13,15] While the strength of a halogen bond seems to be proportional to the magnitude of the σ-hole on the halogen atom, [16] the relationship is much less clear for TrBs. For example, BF_3 has a more intense π-hole than BH_3 but, nevertheless, forms a weaker TrB. [17] The π-hole of BX_3 (X = halogen) is deeper for X atoms with greater electronegativity, yet the corresponding TrB follows an opposite order in TrBs with H_2S and H_2Se. [18] The C(sp^2)-H engages in a stronger hydrogen bond than the C(sp^3)-H, [15] while CH_3BH_2 (sp^3) forms a stronger TrB with NH_3 than CH_2CHBH_2 (sp^2). [11] In the context of cooperativity, the binding distances

of weaker interactions are typically shortened much more than those involved in stronger interactions. [19] Yet, in the TrB cases of HCN-HCN-BF_3 and HCN-XCN-BF_3 (X = halogen), it is the stronger TrB that is contracted the most. [2,20]

Among the range of electron donor types that have been studied within TrBs, [21–25] it is N-bases that are most commonly considered, as in CH_3CN-BF_3, [26] HCN-BF_3, [27] H_3N/Me_3N-BR_3 (R = H, F, Cl), [28] H_3N-$AlMe_3$, [29] HCCCN-BF_3, [30] and Me_3CCN-BF_3. [31] Although O-containing molecules are also good electron donors in hydrogen and halogen bonds, they typically do not participate in TrBs. In one very recent example, however, H_2O binds with TrR_3 (Tr = B, Al, and Ga; R = H, F, Cl, and Br), and the dependence of TrB strength on the R substituent is related to the particular Tr atom: The TrB is strengthened as R becomes more electronegative, but an anomaly appears for Tr = B for the F substituent. [18]

While there has been a certain limited amount of study of chalcogen-containing bases, such as the H_2S and H_2Se analogs of H_2O, [18] there has been no consideration of Te as a potential partner atom in TrBs. Te is a common participant in chalcogen bonds, where it acts as the electron-accepting Lewis acid atom and does so in a stronger manner than its lighter S and Se counterparts. [32–34] There are indications, however, that Te can also act as a base. A concrete example is the chalcogen-chalcogen contact in TeMe(CN)-$TeMe_2$, in which the Te atom of $TeMe_2$ shifts electrons into the antibonding C-Te orbital of TeMe(CN). [35] As a second and very recent example, H_2Te acts as an electron donor as it binds with dihalogen molecules, as in a very strong halogen bond with F_2 (–30 kcal/mol). [36] Replacement of the two H atoms of H_2Te by Me dramatically enhances this halogen bond by as much as a factor of seven. [36]

A central question concerns the ability of Te to act as an electron-donating atom in a different sort of noncovalent bond, in this case the TrB. This is an important matter as Te-containing molecules are relevant to many functional materials, displaying some unconventional and striking chemical/physical properties. [37–39] The central goal of this study is to first establish whether Te can act as an electron donor within the context of a TrB and, if so, what are the limits on the strength of any such bond. As indicated above, there has been no study of this issue up to this point. The next question addresses the way in which the TrB is affected by the nature of the Tr atom, for example, B vs Al vs Ga. How do substituents on either the Te or Tr atom change the properties of the TrB, and can the TrB strength be tuned by appropriate choices? What are the contributing factors to a TrB, and can its strength be predicted based on the depth of the π-hole and/or the negative potential associated with the base? And as another related question, can secondary interactions within a given triel-bonded complex be used as a means to strengthen the overall complexation energy?

The simple unsubstituted H_2Te molecule is considered first as its small size and simplicity will facilitate the analysis. It is paired with a variety of triel-containing Lewis acids, beginning with TrH_3. Then, the three H atoms are replaced by each of three halogen atoms, as in TrF_3, $TrCl_3$, and $TrBr_3$, to determine how these electron-withdrawing substituents affect any TrB. In order to fully address this question, three different Tr atoms are included in the dataset: B, Al, and Ga. The effects of substituents on the Lewis base unit are also considered. H_2Te is replaced by F_2Te, $(CN)_2Te$, $(OH)_2Te$, $(NH_2)_2Te$, and $(CH_3)_2Te$ so as to capture not only electron-withdrawing but also electron-releasing groups. Altogether, the dataset includes 34 different complexes.

2 | THEORETICAL METHODS

The structures of monomers and complexes were optimized at the MP2/aug-cc-pVTZ [40] level. The aug-cc-pVTZ-PP [41,42] basis set with effective core potentials [43] was adopted for Te to account for relativistic effects. All geometries correspond to true minima on the potential energy surface with all positive harmonic frequencies. The interaction energy was calculated as the difference in energy between the complex and the sum of the monomers frozen within the complex. The interaction energies were corrected for basis set superposition error (BSSE) using the Boys-Bernardi counterpoise method. [44] All calculations were carried out with the Gaussian 09 suite of programs. [45]

Molecular electrostatic potentials (MEPs) on the 0.001 au isodensity surfaces were evaluated via the wave function analysis-surface analysis suite (WFA-SAS) [46] at the MP2/aug-cc-pVTZ(PP) level. The AIM topological parameters, including electron density, Laplacian, and total energy density at the bond critical point (BCP), were evaluated with the MultiWFN program. [47] Natural bond orbital (NBO) analysis was carried out at the HF/aug-cc-pVTZ(PP) level to evaluate charge transfer (CT) and interorbital interactions using the NBO 3.0 program. [48] The interaction energy was decomposed into its five components (electrostatic, exchange, repulsion, polarization, and dispersion) using the GAMESS program [49] with the localized molecular orbital-energy decomposition analysis (LMO-EDA) method [50] at the MP2/aug-cc-pVTZ(PP) level.

3 | RESULTS

3.1 | H_2Te-TrR_3

Earlier studies have documented the MEPs surrounding TrR_3 and H_2Te, [24,36] which suggest that the molecules would prefer to come together in the orientation shown in Figure 1. This structure allows the mutual approach of a positive π-hole on the Tr atom and a negatively charged Te lone pair, which can act as an electron donor source in a vacant Tr p-orbital. The depth of the π-hole on each TrR_3 molecule is tabulated as the value of

FIGURE 1 Generalized structure of $H_2Te{\cdot\cdot}TrR_3$ defining geometrical parameters

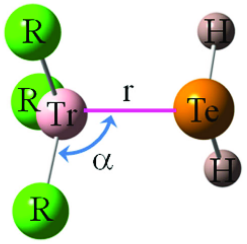

TABLE 1 Values of $V_{s,max}$ (au) for TrR_3 monomers on the ρ = 0.001au isodensity surface

	B	Al	Ga
TrH_3	0.075	0.140	0.115
$TrBr_3$	0.049	0.124	0.113
$TrCl_3$	0.058	0.146	0.132
TrF_3	0.112	0.263	0.207

TABLE 2 Intermolecular distance (r, Å), Te···Tr-R angle (α, deg), interaction energy (E_{int}, kcal/mol), and charge transfer (CT, e) from H_2Te to TrR_3

	r	α	E_{int}	CT
H_2Te-BH_3	2.312	100.7	−20.06	0.524
H_2Te-BBr_3	2.337	104.0	−19.96	0.662
H_2Te-BCl_3	2.421	103.1	−16.14	0.555
H_2Te-BF_3	3.339	92.0	−2.88	0.018
H_2Te-AlH_3	2.893	96.0	−12.93	0.241
H_2Te-$AlBr_3$	2.789	99.9	−21.03	0.333
H_2Te-$AlCl_3$	2.797	99.7	−21.32	0.310
H_2Te-AlF_3	2.805	98.7	−20.50	0.213
H_2Te-GaH_3	2.865	95.9	−11.74	0.255
H_2Te-$GaBr_3$	2.772	100.2	−19.35	0.363
H_2Te-$GaCl_3$	2.773	100.2	−20.42	0.346
H_2Te-GaF_3	2.750	100.1	−22.91	0.273

the maximum of the MEP on a surface corresponding to the ρ = 0.001 au isodensity surface in Table 1, which obeys certain trends. $V_{s,max}$ enlarges in the order B < Ga < Al, although Ga is larger than Al, and there is a pattern that the π-hole deepens as R = Br < Cl < F but that H occupies a variable location in this order, greater than Cl for Tr = B but smaller for Ga.

The optimized values of the r and α parameters of Figure 1 are listed in Table 2, along with the interaction energy and total amount of charge shifted from H_2Te to TrR_3. Regardless of the particular Tr atom, the intermolecular distance is much lower than the sum of van der Waals (vdW) radii of Tr and Te. For the two heavier Tr atoms, r(Tr··Te) is the longest for R = H, while there is not much distinction between the three halogen R atoms. The behavior for B is quite different. In the first place, the intermolecular distances are much shorter, with the singular exception of R = F, which has an anomalously long r = 3.339 Å. Second, r is the shortest for R = H compared to the opposite trend for Al and Ga. There are significant deviations of the α angle from the 90° value within the planar TrR_3 monomers. This deviation appears to correlate with r, in that longer intermolecular distances cause smaller distortions from planarity.

The interaction energies in the penultimate column of Table 2 are fairly large for the most part. With one exception, E_{int} lies in the range between 12 and 23 kcal/mol, thus representing a strong bond. The primary exception is the much weaker bond to BF_3, bound to H_2Te by less than 3 kcal/mol. The interaction energy is closely correlated to r, with shorter TrB distances associated with stronger bonds. For example, the long Te-B distance of 3.339 Å in H_2Te-BF_3 results in an interaction energy of only 2.9 kcal/mol, while the short Te-Ga bond length of 2.75 Å in H_2Te-GaF_3 leads to an interaction energy of 22.9 kcal/mol. There is also a tight connection between r and E_{int} for any particular Tr atom as the R group changes. For Tr = B, the bonding energy drops as R becomes more electronegative: H ∼ Br > Cl > F, but the pattern is quite different for the heavier Tr atoms, where R = H engages in the weakest TrB, and there is only a small dependence on R for the three halogen substituents. The interaction energy of the H_2Te-TrR_3 complex was also calculated at the CCSD(T)/aug-cc-pVTZ level (Table S1). As expected, the more complete

electron correlation correction reduces the interaction energies of most complexes by 1 or 2 kcal/mol. Nevertheless, the variation of interaction energy is similar for both methods. The CTs from base to acid in the last column of Table 2 are quite sizable, particularly for Tr = B, where they exceed 0.5 e. A similar sort of correlation, albeit a bit less quantitative, applies to the comparison of CT with E_{int}. But it might be noted that, even for roughly equivalent interaction energies, CT is consistently larger for Tr = B than for the heavier Tr atoms. We also obtained CT at the HF/cc-pVTZ level (Table S2). The addition of diffuse functions increases CT in most complexes, except H_2Te-BF_3. The CT difference between the two basis sets is very small (<0.03e), and the CT variation is not changed for the different basis sets.

The AIM measures of electron density topology in Table 3 are generally consistent with the above trends. The values of ρ at the BCP in the first column lie in the range of 0.01 to 0.08 au, which are typical of weak to strong noncovalent bonds at either extreme. On the other hand, the negative values of $\nabla^2\rho$ for both H_2Te-BBr_3 and H_2Te-BCl_3 suggest at least a partial covalent bond character, an idea that is bolstered by i) their very large ρ that exceeds 0.07 au and ii) their particularly large CTs of more than 0.5e. But it should be observed that the interaction energies of these two systems, 16 to 20 kcal/mol, are lower than some of the other systems for which $\nabla^2\rho$ is clearly positive.

Another window into the nature of these interactions arises when the total interaction energy is partitioned into its constituent components. The results of such a partition are displayed in Table 4, where it may be seen first that the electrostatic and polarization terms are roughly equivalent. It is interesting that E^{pol} is larger than E^{ele} for the Tr = B systems, whereas the opposite is true for the two larger Tr atoms. While still appreciable, dispersion accounts for a smaller share of the attractive interaction. E^{disp} is roughly three to five times lower than E^{ele}. In terms of absolute values, all attractive terms are considerably larger for the Tr = B complexes, even if the total interaction energy is not. The glaring exception to all of these observations is again H_2Te-BF_3, where the electrostatic term is much the largest, with polarization and dispersion making roughly equal smaller contributions. The total interaction energies of these complexes were also decomposed with a small basis set, such as aug-cc-pVDZ (Table S3). The small basis set has a reverse effect on both E^{ele} and E^{pol}. Namely, E^{ele} becomes larger, but E^{pol} is smaller. Even so, such a small basis set has no effect on the relative variations of both E^{ele} and E^{pol}.

TABLE 3 Electron density (ρ), its Laplacian ($\nabla^2\rho$), and energy density (H) at the intermolecular BCP in H_2Te-TrR_3, all in au

	ρ	$\nabla^2\rho$	H
H_2Te-BH_3	0.0666	0.0607	−0.0476
H_2Te-BBr_3	0.0847	−0.1462	−0.0561
H_2Te-BCl_3	0.0707	−0.1002	−0.0420
H_2Te-BF_3	0.0097	0.0212	0.0003
H_2Te-AlH_3	0.0246	0.0572	−0.0039
H_2Te-$AlBr_3$	0.0344	0.0694	−0.0081
H_2Te-$AlCl_3$	0.0333	0.0698	−0.0076
H_2Te-AlF_3	0.0307	0.0738	−0.0059
H_2Te-GaH_3	0.0345	0.0604	−0.0063
H_2Te-$GaBr_3$	0.0464	0.0502	−0.0127
H_2Te-$GaCl_3$	0.0461	0.0508	−0.0127
H_2Te-GaF_3	0.0473	0.0532	−0.0135

TABLE 4 Electrostatic (E^{ele}), exchange (E^{ex}), repulsion (E^{rep}), polarization (E^{pol}), and dispersion (E^{disp}) energies in H_2Te-TrR_3, all in kcal/mol

	E^{ele}	E^{ex}	E^{rep}	E^{pol}	E^{disp}
H_2Te-BH_3	−40.39	−101.67	188.26	−52.27	−14.17
H_2Te-BBr_3	−67.25	−144.26	284.40	−77.91	−15.01
H_2Te-BCl_3	−53.33	−114.02	222.85	−58.34	−13.44
H_2Te-BF_3	−7.50	−11.33	21.07	−2.42	−2.70
H_2Te-AlH_3	−22.50	−39.08	72.30	−18.32	−5.43
H_2Te-$AlBr_3$	−35.59	−60.06	115.46	−32.86	−8.05
H_2Te-$AlCl_3$	−32.62	−51.45	100.01	−30.42	−7.01
H_2Te-AlF_3	−26.56	−30.09	63.04	−24.77	−2.39
H_2Te-GaH_3	−29.30	−47.55	90.75	−18.51	−7.09
H_2Te-$GaBr_3$	−44.00	−69.49	137.73	−34.33	−9.15
H_2Te-$GaCl_3$	−41.46	−61.31	123.22	−32.80	−8.03
H_2Te-GaF_3	−37.33	−40.99	88.97	−30.80	−2.78

One might expect that the electrostatic components ought to bear some correlation with the depth of the π-hole in the Lewis acid, but any strict correlation is a very weak one indeed, with a linear correlation coefficient R^2 of only 0.2. For example, despite having the lowest values of $V_{s,max}$, the BR_3 acids yield the largest electrostatic energies, with the exception of BF_3 with a very small E^{ele} in contrast with its $V_{s,max}$, which is the largest in the Tr = B series. This poor correspondence is further evidence that these TrBs involve far more than a Coulombic interaction. This conclusion is also confirmed by the worse correlation between $V_{s,max}$ and the total interaction energy (Figure S1).

3.2 | F_2Te-TrR_3

The TrBs involving the H_2Te base are rather strong and involve a substantial amount of covalent character, monomer geometry deformation, and very large CT of as much as 0.5e or more. A weakening of this interaction might allow for another perspective on the bonding, less dependent on these distortions, which could focus better on the noncovalent forces. Replacing the H atoms of the H_2Te base with electron-withdrawing F substituents ought to reduce the negative potential surrounding the Te atom. For example, as documented in Table 5, the $V_{s,min}$ of F_2Te is equal to −0.004 au, compared to −0.022 au for H_2Te. Another effect of the F substitution would be to reduce the accessibility of the Te lone pairs for charge donation to the Lewis acid.

The effects of this weaker base are given in Table 6, which reports the quantities for the F_2Te-TrR_3 complexes, along with their difference relative to the unsubstituted H_2Te-TrR_3. Rather than elongating the TrBs, a shortening is observed in most cases. Even more interesting, the effects on the interaction energy are not uniformly weakening, as might have been anticipated, but are strengthening in more cases than not. (The cases of the AlH_3 and GaH_3 bases are unique in that their interaction with F_2Te causes a drastic change in molecular arrangement. Rather than a Tr··Te TrB, one of the three H atoms of TrH_3 swings around between the Tr and Te atoms and acts as a bridge between them. So, these complexes are not considered further here.)

In order to fully understand the effects of the F substitution of the base, one must bear in mind that this replacement not only affects the magnitude of $V_{s,min}$ but also introduces a pair of σ-holes into the MEP by virtue of the very polar Te-F bonds. The MEPs of H_2Te and F_2Te are displayed in the upper portion of Figure 2, where the red regions indicate the position of these holes, as well as their quantitative value in the form of $V_{s,max}$. It is immediately clear that the σ-hole is much more intense in F_2Te than in H_2Te, with $V_{s,max}$ increasing by a factor of 2.5 from 0.041 to 0.102 au. These σ-holes on F_2Te offer the possibility that an electronegative R atom on TrR_3 could serve as an electron-donating source in a FTe···R chalcogen bond (YB).

As shown in Figure S2, the shorter Te···R distance is 2.559, 2.979, 2.836, 3.616, 3.032, 2.968, 2.852, 2.989, 2.909, and 2.474 Å in F_2Te-BH_3, F_2Te-BBr_3, F_2Te-BCl_3, F_2Te-BF_3, F_2Te-$AlBr_3$, F_2Te-$AlCl_3$, F_2Te-AlF_3, F_2Te-$GeBr_3$, F_2Te-$GaCl_3$, and F_2Te-GaF_3, respectively. Thus, there are indeed

TABLE 5 Values of $V_{s,min}$ and $V_{s,max}$ (au) for R_2Te monomers on the ρ = 0.001 au isodensity surface

	$V_{s,min}$	$V_{s,max}$
H_2Te	−0.022	0.041
F_2Te	−0.004	0.102
$(CN)_2Te$	+0.020	0.103
$(OH)_2Te$	−0.024	0.062
$(NH_2)_2Te$	−0.026	0.025
$(CH_3)_2Te$	−0.035	0.028

TABLE 6 Intermolecular Tr··Te distance (r, Å), interaction energy (E_{int}, kcal/mol), electron density (ρ, au), and charge transfer (CT, e) in F_2Te-TrR_3 complexes, along with their difference (Δ) in comparison with H_2Te-TrR_3 analogs

	r	Δr	E_{int}	ΔE_{int}	ρ	Δρ	CT	ΔCT
F_2Te-BH_3	2.135	−0.177	−31.67	−11.61	0.098	0.032	0.706	0.182
F_2Te-BBr_3	2.213	−0.124	−27.66	−7.70	0.110	0.025	0.685	0.072
F_2Te-BCl_3	2.265	−0.156	−23.16	−7.02	0.098	0.027	0.735	0.130
F_2Te-BF_3	3.347	0.008	−1.80	1.08	0.010	0.000	0.036	0.017
F_2Te-$AlBr_3$	2.722	−0.067	−21.40	−0.37	0.039	0.005	0.312	−0.021
F_2Te-$AlCl_3$	2.738	−0.059	−19.88	−1.44	0.037	0.004	0.320	0.010
F_2Te-AlF_3	2.786	−0.019	−15.89	4.61	0.032	0.001	0.272	0.059
F_2Te-$GaBr_3$	2.693	−0.079	−21.17	−1.82	0.055	0.009	0.339	−0.024
F_2Te-$GaCl_3$	2.703	−0.070	−20.46	−0.04	0.054	0.007	0.365	0.018
F_2Te-GaF_3	2.675	−0.075	−22.08	0.83	0.054	0.007	0.344	0.071

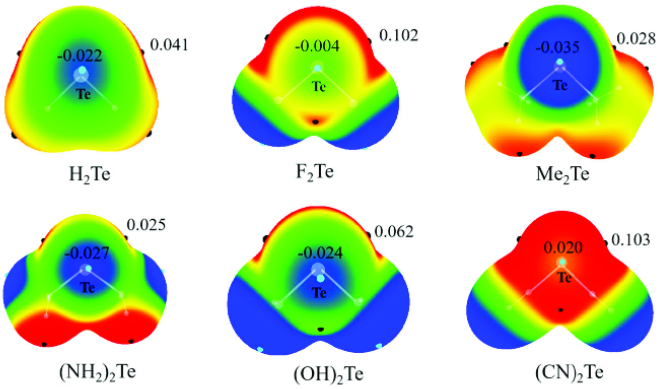

FIGURE 2 Molecular electrostatic potential (MEP) maps on the 0.001 au isodensity surface of Lewis bases. Color ranges, in au, are: red, >0.02; yellow, 0.02-0; green, 0-0.02; blue, <−0.02

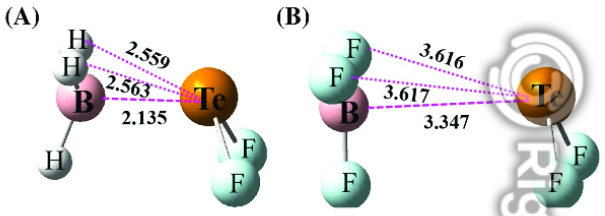

FIGURE 3 Optimized geometries of (A) F_2Te-BH_3 and (B) F_2Te-BF_3

F_2Te-BH_3[a]	6.62	6.74
F_2Te-BBr_3	10.90	10.90
F_2Te-BCl_3	7.48	7.59
F_2Te-BF_3	0.05	0.06
F_2Te-$AlBr_3$	6.81	6.92
F_2Te-$AlCl_3$	3.50	3.42
F_2Te-AlF_3	0	0
F_2Te-$GaBr_3$	0.80	19.76
F_2Te-$GaCl_3$	3.32	3.46
F_2Te-GaF_3	0.59	0.59

[a]$\sigma_{Tr\text{-}H} \rightarrow \sigma^*_{Te\text{-}F}$.

TABLE 7 Second-order perturbation energies $E^{(2)}$ (kcal/mol) for $LP_R \rightarrow \sigma^*_{Te\text{-}F}$ in Tr··R chalcogen bonds

such chalcogen bonds in most of the complexes considered here. An example is illustrated for the F_2Te-BH_3 complex in Figure 3A, where the two molecules reorient in such a way as to place the H atoms roughly along the F-Te bond elongations. In addition to the B···Te TrB of length 2.135, there are a pair of FTe···H chalcogen bonds with R(Te···H) = 2.56 Å. The electron source for these bonds is the set of σ(TrH) bond orbitals. In the more general case of TrX_3, it is the halogen atom lone pairs that serve in this capacity. The magnitudes of these auxiliary YBs can be gauged by NBO values of second-order perturbation energies $E^{(2)}$ for CT from the halogen lone pairs to the σ*(TeF) antibonding orbital. Table 7 lists these quantities for all of the various complexes. (Note that, even without the halogen lone pairs, the BH_3 molecule can also engage in these YBs, employing the σ[BH] bonding orbitals as an alternate source of electron density.) In most cases, the two YBs are roughly equivalent to one another. An exception is the F_2Te-$GaBr_3$ system, where the molecules reorient so that one is far stronger than the other. It might also be noted that the TrF_3 molecules form very weak YBs, with $E^{(2)}$ lower than 1 kcal/mol. An example is illustrated in Figure 3B, which shows less reorientation to accommodate the weak F···Te interactions. For example, the θ(F···TeF) angles in Figure 3B are 118°, quite far from the linearity of an optimum YB. The comparable angles in Figure 3A are 133°, much closer to the preferred angle. The existence of a chalcogen bond in F_2Te-TrR_3 (Tr = B, Al, and Ga; R = Cl and Br) can also be further confirmed with the NCI color regions between the Te and R atoms (Figure S3).

So, the effect of the F substitution is a net result of two counteracting effects. On one hand, this substitution weakens the MEP minimum on the base, which would likewise weaken the TrB. But the total interaction is strengthened by the introduction of stabilizing YBs, which bring the

TABLE 8 Intermolecular distance (r, Å), Te···Tr-H angle (α, deg), interaction energy (E_{int}, kcal/mol), and charge transfer (CT, e) from R'_2Te to BH_3

	r	α	E_{int}	CT
H_2Te-BH_3	2.312	100.7	−20.06	0.524
F_2Te-BH_3	2.337	104.0	−31.67	0.706
$(CN)_2Te$-BH_3	2.296	103.7	−13.46	0.457
$(OH)_2Te$-BH_3	2.179	99.9	−29.21	0.655
$(NH_2)_2Te$-BH_3	2.227	101.5	−32.39	0.640
$(CH_3)_2Te$-BH_3	2.259	102.8	−31.83	0.601

TABLE 9 Electrostatic (E^{ele}), exchange (E^{ex}), repulsion (E^{rep}), polarization (E^{pol}), and dispersion (E^{disp}) energies in R'_2Te-BH_3, all in kcal/mol

	E^{ele}	E^{ex}	E^{rep}	E^{pol}	E^{disp}
H_2Te-BH_3	−40.39	−101.67	188.26	−52.27	−14.17
F_2Te-BH_3	−65.25	−146.28	282.62	−84.40	−18.66
$(CN)_2Te$-BH_3	−33.45	−95.40	179.61	−48.67	−15.74
$(OH)_2Te$-BH_3	−57.15	−131.57	250.19	−73.57	−17.36
$(NH_2)_2Te$-BH_3	−58.04	−127.27	238.34	−69.09	−16.58
$(CH_3)_2Te$-BH_3	−54.12	−121.00	224.62	−65.21	−16.36

two molecules into closer proximity. Moreover, as each molecule is serving simultaneously as both electron donor and acceptor, any such YB is likely to mutually reinforce the TrB in a positive cooperativity scenario.

The way in which these competing effects play out is integral to the interpretation of Table 6. For the F_2Te-TrR_3 complexes with R = H, Br, or Cl, the chalcogen bonds strengthen the overall interaction, enhancing the interaction energy and contracting the intermolecular separation. As the Te and Tr atoms are pulled closer together, their BCP density is increased. These enhancements are particularly large for the F_2Te-BH_3 dimers, which can be traced to the especially strong YBs delineated in Table 7. In the cases where R = F, there is no such chalcogen bond to counter the weakening of the Tr··Te TrB, so there is a mild overall reduction in E_{int}. As the total intermolecular CT is a mix of transfer in both directions, TrB vs YB, the values of ΔCT in Table 6 are similarly of variable signs. As a last point, the compilation of Wiberg bond indices (WBI) in Table S4 reaffirms the strengthening of the TrB caused by the F substitution of the base.

The Te atom of F_2Te plays a dual role of both a Lewis base in the TrB and acid in the YB, which is a factor in the mutual cooperativity of these two bonds. There is precedent for this situation in the literature in that a similar dual role was also reported for F_2CSe, [51] where the Se atom forms a chalcogen bond and a regium bond simultaneously.

3.3 | R'_2Te-BH_3

Given the interesting interplay between opposing effects upon F substitution of H_2Te, it would be interesting to see if similar reasoning applies to other substitutions. As choices for this role, electron-withdrawing CN was compared with electron-releasing OH, NH_2, and CH_3. The BH_3 unit was taken as the model TrB donor. The exchange of F for one of these other substituents removes the presence of the chalcogen bonds, so one can achieve a purer examination of the TrB itself.

The geometric and other parameters of these R'_2Te-BH_3 complexes are given in Table 8, where it may be seen that most of the R′ substituents enhance the interaction energy relative to H_2Te, with the exception of CN. The same pattern may be seen in the total CT in the last column of Table 8. This ordering can be compared with the magnitude of the values of $V_{s,min}$ in Table 5. While electron-withdrawing R′ = F and CN both reduce the negative value of this parameter, it is made a bit more negative for the other electron-releasing substituents. One may thus understand the stronger TrBs for the latter three R′, as well as the weakened bond for R′ = CN. The same would be true for R′ = F were it not for the two chalcogen bonds that occur in this complex. Many of these same rules apply to the individual energy components for these complexes listed in Table 9. Although E^{ele}, E^{pol}, and E^{disp} all grow larger for R′ = OH, NH_2, and CH_3, as well as F, the opposite is seen for CN (with the minor exception of a slightly higher dispersion energy).

4 | DISCUSSION

There is a general rule that withdrawing groups in the electron acceptor will strengthen an acid-base interaction. This concept is valid for some of the systems considered here but not all. This rule is inverted in the case of the BR_3 acids, where the order of interaction energy decreases in the

order H > Br > Cl > F. The rule is a bit more valid for the AlR_3 acids, although there is little distinction between the three halogen atoms as R substituents. In the converse of this idea, one would anticipate that electron-withdrawing substituents on the base ought to weaken the interaction. However, this rule, too, is not steadfastly adhered to. It is true that electron-withdrawing F and CN both weaken the negative region of the potential around the Te lone pairs, while electron-releasing OH, NH_2, and CH_3 make this slightly more negative. These small changes are reflected in an (disproportionately large) increase in the interaction energy for the latter substituents, and CN weakens the interaction. However, the interaction of F_2Te with BH_3 yields an increased interaction energy, despite the reduced negative potential. This apparent paradox is resolved by recalling that each highly electron-withdrawing F substituent induces a positive σ-hole on the Te atom, which can then engage in an FTe··X chalcogen bond with the halogen substituents on TrX_3 or even with the σ(BH) bonding orbitals of TrH_3. So, the full complexation energy includes not only a TrB but also a pair of chalcogen bonds.

As indicated in Table 5, the electron-withdrawing ability of CN is strong enough that the MEP at the Te lone pair position is in fact positive, at least on the ρ = 0.001 au isodensity surface. Nevertheless, $(CN)_2Te$ still engages in a fairly strong TrB with BH_3, with E_{int} up to −13.46 kcal/mol. This sort of phenomenon has precedent in the literature. Even after depressing the negative potential near the C=C bond of $C_2(CN)_2$, $C_2(CN)_2$ still acts as an electron donor in a strong regium bond with AuCN. [13] Similarly, for the halogen bond, which typically requires a positive σ-hole on the halogen atom, [52] there are cases where such a bond is formed even in the absence of such a region on the halogen atom, as when IAu interacts with HArF. [53]

The electron donation of the Te lone pairs observed here in TrBs fits into a pattern where a similar phenomenon has been observed in hydrogen, halogen, and regium bonds. [36,54] Another issue regarding Te is that, in most cases, hydrogen bonding is stronger than halogen bonding for a common electron donor. However, the reverse of this order was observed in complexes between H_2Te and 6-OX-fulvene (X = H, Cl, Br, and I). [54] Moreover, the halogen bond is particularly strong for X = Cl, much stronger than the corresponding hydrogen bond. [54] A similar trend was also noted in the complexes between H_2Te and XF (X = H, Cl, Br, and I). [36] The interaction energy was −4 kcal/mol for the hydrogen-bonded complex of H_2Te-HF;[36] thus, the Te atom of H_2Te has stronger affinity to the triel atom. This conclusion holds true when halogen and triel atoms are compared as the interaction energy between H_2Te and XF seldom exceeds −14 kcal/mol.[36]

Chalcogen atoms other than Te also participate in TrBs as an electron donor, which facilitates a comparison. Heavier chalcogen atoms generally lead to a weaker TrB, which is usually attributed to their lesser electronegativity and accompanying reduced potential at the site of their lone pairs. On the other hand, H_2Te engages in a slightly stronger TrB with Br_3Ga than do H_2S and H_2Se, with interaction energies of −18.5 and −18.7 kcal/mol, respectively. [18] This general order is also true for the hydrogen bond, but more unusual results are found for the halogen bond. [54] H_2Te forms a stronger halogen bond with 6-OX-fulvene (X = Cl, Br, and I) than do lighter chalcogen atoms. [54]

The way in which the identity of the R substituent of TrR_3 influences triel bonding strength depends on the particular Tr atom. With the increase of R electronegativity, the TrB becomes stronger for Al and Ga but weaker for B. [36] This dependence is usually true for other chalcogen electron donors as well. On the other hand, E_{int} has little dependence on R in the H_2Te-AlR_3 series. The π-hole intensity of TrR_3 increases in the order of B < Ga < Al, but the interaction energy does not necessarily follow this same order. The TrB is stronger in the Ga < Al < B order for TrH_3, Ga < B < Al for $TrCl_3$, and B < Al < Ga for TrF_3.

5 | CONCLUSIONS

The TrBs in the complexes with Te serving as an electron donor in the base molecule are of variable strength, ranging from 3 to 23 kcal/mol. Most notable are the surprising substituent effects in these $R'_2Te··TrR_3$ complexes. While increasing electronegativity of the R substituent on the acid leads to a strengthened TrB for Tr = Ga, and Al to a lesser extent, this trend is reversed for Tr = B, where H_2Te-BF_3 is the most weakly bound of all. Adding F substituents to the base reduces the magnitude of the negative potential at the site of the Te lone pairs. But contrary to expectation, this same substitution nevertheless strengthens the interaction with the Lewis acids. The enhancement of TrB in F_2Te-TrR_3 can be evidenced by not only the shortening of Te···Tr distance but also the increase of electron density at the Te···Tr BCP, as well as the WBI of Te-Tr bond. This strengthening is caused by the formation of new stabilizing secondary interactions in F_2Te-TrR_3, in the form of FTe··R chalcogen bonds, which are facilitated by the introduction of positive σ-holes near the Te atoms along the extensions of the F-Te covalent bonds. Curiously, F substituents on the acid are unable to participate in these chalcogen bonds, so F_2Te-TrF_3 complexes are weakened by the F substitution on the base. Placement of generic electron-releasing R′ substituents OH, NH_2, and CH_3 on the base enhances the negative potential around the Te atom of R'_2Te, and thereby strengthens the interaction. The opposite occurs for the electron-withdrawing R′ = CN substituent.

ACKNOWLEDGMENTS

This work was supported by the Science and Technology Innovation Fund of Yantai University (YDZD2011) and the National Natural Science Foundation of China (21573188).

AUTHOR CONTRIBUTIONS

Ruijing Wang: Data curation; formal analysis; investigation; visualization; writing-original draft. **Canlin Luo:** Data curation; formal analysis; investigation; validation. **Qingzhong Li:** Conceptualization; funding acquisition; project administration; resources; software; validation; writing-review and editing. **Steve Scheiner:** Conceptualization; formal analysis; project administration; validation; writing-review and editing.

ORCID

Qingzhong Li https://orcid.org/0000-0003-1486-6772

REFERENCES

[1] S. J. Grabowski, *ChemPhysChem* **2014**, *15*, 2985.
[2] D. Fiacco, K. Leopold, *J. Phys. Chem. A* **2003**, *107*, 2808.
[3] J. S. Murray, P. Lane, T. Clark, K. E. Riley, P. Politzer, *J. Mol. Model.* **2012**, *18*, 541.
[4] M. Michalczyk, W. Zierkiewicz, S. Scheiner, *ChemPhysChem* **2018**, *19*, 3122.
[5] J. Grotewold, E. A. Lissi, A. E. Villa, *J. Chem. Soc. A* **1966**, *0*, 1034.
[6] J. Grotewold, E. A. Lissi, A. E. Villa, *J. Chem. Soc. A* **1966**, *0*, 1038.
[7] H. Kameo, Y. Baba, S. Sakaki, Y. Tanaka, H. Matsuzaka, *Inorg. Chem.* **2020**, *59*, 4282.
[8] S. J. Grabowski, *Crystals* **2019**, *9*, 503.
[9] S. J. Grabowski, *Phys. Chem. Chem. Phys.* **2017**, *19*, 29742.
[10] L. Gao, Y. Zeng, X. Zhang, L. Meng, *J. Comput. Chem.* **2016**, *37*, 1321.
[11] Z. Xu, Y. Li, *J. Mol. Model.* **2019**, *25*, 219.
[12] M. Liu, H. Zhuo, Q. Li, W. Li, J. Cheng, *J. Mol. Model.* **2016**, *22*, 10.
[13] J. Zhang, Z. Wang, S. Liu, J. Cheng, W. Li, Q. Li, *Appl. Organomet. Chem.* **2019**, *33*, e4806.
[14] S. Yourdkhani, T. Korona, N. L. Hadipour, *J. Comput. Chem.* **2015**, *36*, 2412.
[15] X. An, H. Liu, Q. Li, B. Gong, J. Cheng, *J. Phys. Chem. A* **2008**, *112*, 5258.
[16] K. E. Riley, J. S. Murray, J. Fanfrlík, J. Řezáč, R. J. Solá, M. C. Concha, P. Politzer, *J. Mol. Model.* **2011**, *17*, 3309.
[17] S. J. Grabowski, *ChemPhysChem* **2015**, *16*, 1470.
[18] Z. Chi, Q. Li, H. Li, *Int. J. Quantum Chem.* **2020**, *120*, e26046.
[19] Q. Li, R. Li, X. Liu, W. Li, J. Cheng, *ChemPhysChem* **2012**, *13*, 1205.
[20] Q. Tang, Q. Li, *Mol. Phys.* **2015**, *113*, 3809.
[21] S. J. Grabowski, *Molecules* **2015**, *20*, 11297.
[22] A. Bauzá, A. Frontera, *Theor. Chem. Acc.* **2017**, *136*, 37.
[23] J. Zhang, Y. Wei, W. Li, J. Cheng, Q. Li, *Appl. Organomet. Chem.* **2018**, *32*, e4367.
[24] Z. Chi, W. Dong, Q. Li, X. Yang, S. Scheiner, S. Liu, *Int. J. Quant. Chem.* **2019**, *119*, e25867.
[25] M. D. Esrafili, F. Mohammadian-Sabet, *Struct. Chem.* **2016**, *27*, 1157.
[26] M. A. Dvorak, R. S. Ford, R. D. Suenram, F. J. Lovas, K. R. Leopold, *J. Am. Chem. Soc.* **1992**, *114*, 108.
[27] W. A. Burns, K. R. Leopold, *J. Am. Chem. Soc.* **1993**, *115*, 11622.
[28] V. Jonas, G. Frenking, M. T. Reetzi, *J. Am. Chem. Soc.* **1994**, *116*, 8141.
[29] J. Muller, U. Ruschewitz, O. Indris, H. Hartwig, W. Stahl, *J. Am. Chem. Soc.* **1999**, *121*, 4647.
[30] E. R. T. Kerstel, H. Pate, T. F. Mentel, X. Yang, G. Stoles, *J. Chem. Phys.* **1994**, *101*, 2763.
[31] J. A. Phillips, D. J. Giesen, N. P. Wells, J. A. Halfen, C. C. Knutson, J. P. Wiass, *J. Phys. Chem. A* **2005**, *109*, 8199.
[32] S. Tsuzuki, N. Sato, *J. Phys. Chem. B* **2013**, *117*, 6849.
[33] G. E. Garrett, E. I. Carrera, D. S. Seferos, M. S. Taylor, *Chem. Commun.* 2016, *52*, 9881.
[34] A. Panda, R. N. Behera, *J. Hazard. Mater.* **2014**, *269*, 2.
[35] C. Bleiholder, R. Gleiter, D. B. Werz, H. Kölppel, *Inorg. Chem.* **2007**, *46*, 2249.
[36] R. Wang, Z. Cheng, Q. Li, S. A. C. McDowell, *Appl. Organomet. Chem.* **2020**, *34*, e5468.
[37] Y. Liu, W. Wu, W. A. Goddard III., *J. Am. Chem. Soc.* **2018**, *140*, 2550.
[38] J. Qiao, Y. Pan, F. Yang, C. Wang, Y. Chai, W. Ji, *Sci. Bull.* **2018**, *63*, 159.
[39] K. Xu, X. Liu, J. Liang, J. Cai, K. Zhang, Y. Lu, X. Wu, M. Zhu, Y. Liu, Y. Zhu, G. Wang, Y. Qian, *ACS Energy Lett.* **2018**, *8*, 420.
[40] A. K. Wilson, D. E. Woon, K. A. Peterson, T. H. Dunning Jr., *J. Chem. Phys.* **1999**, *110*, 7667.
[41] K. A. Peterson, B. C. Shepler, D. Figgen, H. Stoll, *J. Phys. Chem. A* **2006**, *110*, 13877.
[42] K. A. Peterson, D. Figgen, M. Dolg, H. Stoll, *J. Chem. Phys.* **2007**, *126*, 124101.
[43] B. P. Pritchard, D. Altarawy, B. T. Didier, T. Gibson, T. L. Windus, *J. Chem. Inf. Model.* **2019**, *59*, 4814.
[44] S. F. Boys, F. D. Bernardi, *Mol. Phys.* **1970**, *19*, 553.
[45] M. J. Frisch, G. W. Trucks, H. B. Schlegel, G. E. Scuseria, M. A. Robb, J. R. Cheeseman, G. Scalmani, V. Barone, B. Mennucci, G. A. Petersson, H. Nakatsuji, M. Caricato, X. Li, H. P. Hratchian, A. F. Izmaylov, J. Bloino, G. Zheng, J. L. Sonnenberg, M. Hada, M. Ehara, K. Toyota, R. Fukuda, J. Hasegawa, M. Ishida, T. Nakajima, Y. Honda, O. Kitao, H. Nakai, T. Vreven, J. J. A. Montgomery, J. E. Peralta, F. Ogliaro, M. Bearpark, J. J. Heyd, E. Brothers, K. N. Kudin, V. N. Staroverov, R. Kobayashi, J. Normand, K. Raghavachari, A. Rendell, J. C. Burant, S. S. Iyengar, J. Tomasi, M. Cossi, N. Rega, J. M. Millam, M. Klene, J. E. Knox, J. B. Cross, V. Bakken, C. Adamo, J. Jaramillo, R. Gomperts, R. E. Stratmann, O. A. Yazyev, J. Austin, R. Cammi, C. Pomelli, J. W. Ochterski, R. L. Martin, K. Morokuma, V. G. Zakrzewski, G. A. Voth, P. Salvador, J. J. Dannenberg, S. A. Dapprich, D. Daniels, O. Farkas, J. B. Foresman, J. V. Ortiz, J. Cioslowski, D. J. Fox, *Gaussian 09, Revision A.02*, Gaussian, Inc., Wallingford, CT **2009**.
[46] F. A. Bulat, A. Toro-Labbé, T. Brinck, J. S. Murray, P. Politzer, *J. Mol. Model.* **2010**, *16*, 1679.
[47] T. Lu, F. Chen, *J. Chem. Phys.* **2012**, *33*, 580.
[48] A. E. Reed, L. A. Curtiss, F. Weinhold, *Chem. Rev.* **1988**, *88*, 899.

[49] M. W. Schmidt, K. K. Baldridge, J. A. Boatz, S. T. Elbert, M. S. Gordon, J. H. Jensen, S. Koseki, N. Matsunaga, K. A. Nguyen, S. Su, *J. Comput. Chem.* **1993**, *14*, 1347.
[50] P. Su, H. Li, *J. Chem. Phys.* **2009**, *131*, 014102.
[51] X. Guo, Y. Yang, Q. Li, H. Li, *J. Chem. Phys.* **2016**, *144*, 114306.
[52] T. Clark, M. Hennemann, J. S. Murray, P. Politzer, *J. Mol. Model.* **2007**, *13*, 291.
[53] R. Wang, Q. Li, S. Scheiner, *Appl. Organomet. Chem.* **2020**, *34*, e5891.
[54] M. Hou, Q. Li, S. Scheiner, *ChemPhysChem* **2019**, *20*, 1978.

SUPPORTING INFORMATION

Additional supporting information may be found online in the Supporting Information section at the end of this article.

How to cite this article: Wang R, Luo C, Li Q, Scheiner S. Unusual substituent effects in the Tr···Te triel bond. *Int J Quantum Chem*. 2021; 121:e26526. https://doi.org/10.1002/qua.26526